

## Results of the $^{244}\text{Cm}$ , $^{246}\text{Cm}$ and $^{248}\text{Cm}$ neutron-induced capture cross sections measurements at EAR1 and EAR2 of the n\_TOF facility

V. Alcayne<sup>1,\*</sup>, E. Mendoza<sup>1</sup>, D. Cano-Ott<sup>1</sup>, A. Kimura<sup>2</sup>, O. Aberle<sup>3</sup>, S. Amaducci<sup>4,5</sup>, J. Andrzejewski<sup>6</sup>, L. Audouin<sup>7</sup>, V. Babiano-Suarez<sup>8</sup>, M. Bacak<sup>3,9,10</sup>, M. Barbagallo<sup>3,11</sup>, V. Bécaries<sup>1</sup>, F. Bečvář<sup>12</sup>, G. Bellia<sup>4,5</sup>, E. Berthoumieux<sup>10</sup>, J. Billowes<sup>13</sup>, D. Bosnar<sup>14</sup>, A. S. Brown<sup>15</sup>, M. Busso<sup>16,17</sup>, M. Caamaño<sup>18</sup>, L. Caballero<sup>8</sup>, M. Calviani<sup>3</sup>, F. Calviño<sup>19</sup>, A. Casanovas<sup>19</sup>, F. Cerutti<sup>3</sup>, Y. H. Chen<sup>7</sup>, E. Chiaveri<sup>13,20,3</sup>, N. Colonna<sup>11</sup>, G. P. Cortés<sup>19</sup>, M. A. Cortés-Giraldo<sup>20</sup>, L. Cosentino<sup>4</sup>, S. Cristallo<sup>16,21</sup>, L. A. Damone<sup>11,22</sup>, M. Diakaki<sup>23</sup>, M. Dietz<sup>24</sup>, C. Domingo-Pardo<sup>8</sup>, R. Dressler<sup>25</sup>, E. Dupont<sup>10</sup>, I. Durán<sup>18</sup>, Z. Eleme<sup>26</sup>, B. Fernández-Domínguez<sup>18</sup>, A. Ferrari<sup>3</sup>, I. Ferro-Gonçalves<sup>27</sup>, P. Finocchiaro<sup>4</sup>, V. Furman<sup>28</sup>, R. Garg<sup>24</sup>, A. Gawlik<sup>6</sup>, S. Gilardoni<sup>3</sup>, T. Glodariu<sup>29</sup>, K. Göbel<sup>30</sup>, E. González-Romero<sup>1</sup>, C. Guerrero<sup>20</sup>, F. Gunsing<sup>10</sup>, S. Heinitz<sup>25</sup>, J. Heyse<sup>31</sup>, D. G. Jenkins<sup>15</sup>, E. Jericha<sup>9</sup>, Y. Kadi<sup>3</sup>, F. Käppeler<sup>32</sup>, N. Kivel<sup>25</sup>, M. Kokkoris<sup>23</sup>, Y. Kopatch<sup>28</sup>, M. Krtička<sup>12</sup>, D. Kurtulgil<sup>30</sup>, I. Ladarescu<sup>8</sup>, C. Lederer-Woods<sup>24</sup>, J. Lerendegui-Marco<sup>20</sup>, S. Lo Meo<sup>33,34</sup>, S.-J. Lonsdale<sup>24</sup>, D. Macina<sup>3</sup>, A. Manna<sup>34,35</sup>, T. Martínez<sup>1</sup>, A. Masi<sup>3</sup>, C. Massimi<sup>34,35</sup>, P. F. Mastinu<sup>36</sup>, M. Mastromarco<sup>3,13</sup>, F. Matteucci<sup>37,38</sup>, E. Mauger<sup>25</sup>, A. Mazzone<sup>11,39</sup>, A. Mengoni<sup>33,34</sup>, V. Michalopoulou<sup>23</sup>, P. M. Milazzo<sup>37</sup>, F. Mingrone<sup>3</sup>, A. Musumarra<sup>4,5</sup>, A. Negret<sup>29</sup>, R. Nolte<sup>40</sup>, F. Ogállar<sup>41</sup>, A. Oprea<sup>29</sup>, N. Patronis<sup>26</sup>, A. Pavlik<sup>42</sup>, J. Perkowski<sup>6</sup>, L. Piersanti<sup>16,21</sup>, I. Porras<sup>41</sup>, J. Praena<sup>41</sup>, J. M. Quesada<sup>20</sup>, D. Radeck<sup>40</sup>, D. Ramos Doval<sup>7</sup>, R. Reifarth<sup>30</sup>, D. Rochman<sup>25</sup>, C. Rubbia<sup>3</sup>, M. Sabaté-Gilarte<sup>20,3</sup>, A. Saxena<sup>43</sup>, P. Schillebeeckx<sup>31</sup>, D. Schumann<sup>25</sup>, A. G. Smith<sup>13</sup>, N. Sosnin<sup>13</sup>, A. Stamatopoulos<sup>23</sup>, G. Tagliente<sup>11</sup>, J. L. Tain<sup>8</sup>, Z. Talip<sup>25</sup>, A. E. Tarifeño-Saldivia<sup>19</sup>, L. Tassan-Got<sup>3,23,7</sup>, P. Torres-Sánchez<sup>41</sup>, A. Tsinganis<sup>3</sup>, J. Ulrich<sup>25</sup>, S. Urlass<sup>3,44</sup>, S. Valenta<sup>12</sup>, G. Vannini<sup>34,35</sup>, V. Variale<sup>11</sup>, P. Vaz<sup>27</sup>, A. Ventura<sup>34</sup>, V. Vlachoudis<sup>3</sup>, R. Vlastou<sup>23</sup>, A. Wallner<sup>45</sup>, P. J. Woods<sup>24</sup>, T. J. Wright<sup>13</sup>, and P. Žugec<sup>14</sup>

<sup>1</sup>Centro de Investigaciones Energéticas Medioambientales y Tecnológicas (CIEMAT),Spain

<sup>2</sup>Japan Atomic Energy Agency (JAEA), Tokai-mura, Japan

<sup>3</sup>European Organization for Nuclear Research (CERN), Switzerland

<sup>4</sup>INFN Laboratori Nazionali del Sud, Catania, Italy

<sup>5</sup>Dipartimento di Fisica e Astronomia, Università di Catania, Italy

<sup>6</sup>University of Lodz, Poland

<sup>7</sup>IPN, CNRS-IN2P3, Univ. Paris-Sud, Université Paris-Saclay, F-91406 Orsay Cedex,France

<sup>8</sup>Instituto de Física Corpuscular, CSIC - Universidad de Valencia, Spain

<sup>9</sup>Technische Universität Wien, Austria

<sup>10</sup>CEA Saclay, Irfu, Université Paris-Saclay, Gif-sur-Yvette, France

<sup>11</sup>Istituto Nazionale di Fisica Nucleare, Bari, Italy

<sup>12</sup>Charles University, Prague, Czech Republic

<sup>13</sup>University of Manchester, United Kingdom

<sup>14</sup>Department of Physics, Faculty of Science, University of Zagreb, Croatia

<sup>15</sup>University of York, United Kingdom

<sup>16</sup>Istituto Nazionale di Fisica Nucleare, Perugia, Italy

<sup>17</sup>Dipartimento di Fisica e Geologia, Università di Perugia, Italy

<sup>18</sup>University of Santiago de Compostela, Spain

<sup>19</sup>Universitat Politècnica de Catalunya, Spain

<sup>20</sup>Universidad de Sevilla, Spain

<sup>21</sup>Istituto Nazionale di Astrofisica - Osservatorio Astronomico d'Abruzzo, Italy

<sup>22</sup>Dipartimento di Fisica, Università degli Studi di Bari, Italy

<sup>23</sup>National Technical University of Athens, Greece

<sup>24</sup>School of Physics and Astronomy, University of Edinburgh, United Kingdom

<sup>25</sup>Paul Scherrer Institut (PSI), Villigen, Switzerland

<sup>26</sup>University of Ioannina, Greece

<sup>27</sup>Instituto Superior Técnico, Lisbon, Portugal

<sup>28</sup>Joint Institute for Nuclear Research (JINR), Dubna, Russia

<sup>29</sup>Horia Hulubei National Institute of Physics and Nuclear Engineering (IFIN-HH),Bucharest

<sup>30</sup>Goethe University Frankfurt, Germany

<sup>31</sup>European Commission, Joint Research Centre, Geel, Retieseweg 111, B-2440 Geel,Belgium

<sup>32</sup>Karlsruhe Institute of Technology, Campus North, IKP, 76021 Karlsruhe, Germany

<sup>33</sup>Agenzia nazionale per le nuove tecnologie, l'energia e lo sviluppo economico sostenibile (ENEA), Bologna, Italy

<sup>34</sup>Istituto Nazionale di Fisica Nucleare, Sezione di Bologna, Italy

<sup>35</sup>Dipartimento di Fisica e Astronomia, Università di Bologna, Italy

<sup>36</sup>Istituto Nazionale di Fisica Nucleare, Sezione di Legnaro, Italy

<sup>37</sup>Istituto Nazionale di Fisica Nucleare, Trieste, Italy

<sup>38</sup>Dipartimento di Fisica, Università di Trieste, Italy

<sup>39</sup>Consiglio Nazionale delle Ricerche, Bari, Italy

<sup>40</sup>Physikalisch-Technische Bundesanstalt (PTB), Bundesallee 100, 38116 Braunschweig, Germany

<sup>41</sup>University of Granada, Spain

<sup>42</sup>University of Vienna, Faculty of Physics, Vienna, Austria

<sup>43</sup>Bhabha Atomic Research Centre (BARC), India

<sup>44</sup>Helmholtz-Zentrum Dresden-Rossendorf, Germany

<sup>45</sup>Australian National University, Canberra, Australia

**Abstract.** Accurate neutron capture cross section data for minor actinides (MAs) are required to estimate the production and transmutation rates of MAs in light water reactors, critical fast reactors like Gen-IV systems, and other innovative reactor systems such as accelerator driven systems (ADS). In particular,  $^{244}\text{Cm}$ ,  $^{246}\text{Cm}$  and  $^{248}\text{Cm}$  play a role in the transport, storage and transmutation of the nuclear waste of the current nuclear reactors, due to the contribution of these isotopes to the radiotoxicity, neutron emission, and decay heat in the spent nuclear fuel. Also, capture reactions in these Cm isotopes open the path for the formation of heavier elements. In this work, the results of the capture cross section measurement on  $^{244}\text{Cm}$ ,  $^{246}\text{Cm}$  and  $^{248}\text{Cm}$  performed at the CERN n\_TOF facility are presented. It is important to notice that the Cm samples used in the experiment at n\_TOF have been used previously in an experiment at J-PARC, this experiment and the previous one done in the 70s with a nuclear explosion were the only previous capture experiments for these isotopes. At n\_TOF, the capture cross section measurements of  $^{244}\text{Cm}$ ,  $^{246}\text{Cm}$  and  $^{248}\text{Cm}$  were performed at the 20 m vertical flight path (EAR2) with three  $\text{C}_6\text{D}_6$  total energy detectors. In addition, the cross section of  $^{244}\text{Cm}$  was measured at the 185 m flight path (EAR1) with a Total Absorption Calorimeter (TAC). The combination of measurements in EAR1 and EAR2 has contributed to controlling and reducing the systematic uncertainties in the results. The compatibility of the different measurements performed and the techniques to obtain the results are presented in this paper as well as the procedure to obtain the resonance parameters.

## 1 Introduction

The safe and efficient management of the high-level waste produced in the operation of nuclear reactors requires more accurate nuclear data. In particular, inventory calculations of the spent nuclear fuel (SNF) and the derived magnitudes such as the decay heat, radiotoxicity or neutron and gamma dose, among others, rely on the accuracy of neutron induced reaction cross sections ruling the burn-up in the reactor. The Cm isotopes require special attention due to their various implications along the fuel cycle. For instance,  $^{244}\text{Cm}$  is responsible for  $\sim 10\%$  of the radiotoxicity and the decay heat in the spent nuclear fuel in a Light Water Reactor (LWR) during the first fifteen years after unloading the SNF from the reactor. Furthermore, the neutron emission in the spent fuel is dominated by the  $^{244}\text{Cm}$  and  $^{246}\text{Cm}$  spontaneous fission during the first  $10^4$  years of disposal, see Figure 1. For LWR sensitivity analyses performed in [1] indicate that uncertainties in the  $^{244}\text{Cm}$  capture cross section need to be reduced to 4.1% between 4 and 22.6 eV and 14.4% between 22.6 and 454 eV. Last, but not least, more accurate knowledge of the capture cross sections of  $^{244}\text{Cm}$ ,  $^{246}\text{Cm}$  and  $^{248}\text{Cm}$  (hereafter  $^{244,246,248}\text{Cm}$ ) is required for improving the calculations on the formation of heavier isotopes such as Bk, Cf and other Cm isotopes.

There are only three previous capture measurements of these isotopes, the one performed in 1969 using the neutrons of an underground nuclear explosion [3], and the most recent ones performed at J-PARC with the same set

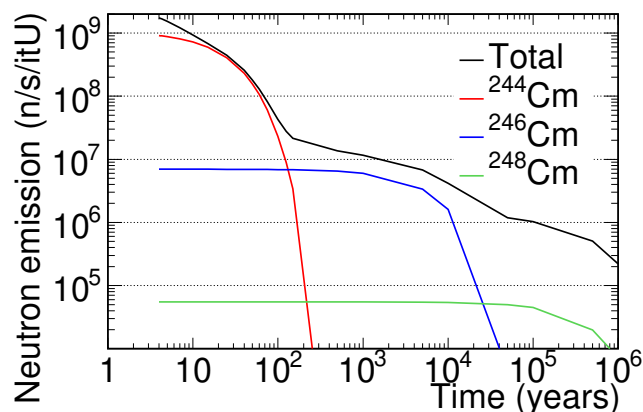


**Figure 1.** Neutron emission of the spent fuel per initial ton of uranium. The calculations have been done with ORIGEN2 [2] for a PWR with a 50 GWd/tU burnup after four years in the spent fuel pool

of samples by Kimura *et al.* in 2010 [4] and by Kawase *et al.* in 2021 [5].

## 2 The experiment

The  $^{244,246,248}\text{Cm}$  cross section has been measured at the n\_TOF spallation neutron-time-of-flight facility at CERN. In order to reduce the systematic uncertainties and to cross-check the results the measurements were performed in two experimental areas, with two different detectors and

\*e-mail: victor.alcayne@ciemat.es

using two different samples. The experiment was performed in Experimental Area 1 (EAR1) located horizontally at 185 m from the target [6] and in Experimental Area 2 (EAR2) located at 21 m vertically [7].

The samples used in the experiment were provided by the Japan Atomic Energy Agency (JAEA), the same batch material has been used in the previous experiments at J-PARC [4, 5]. Sample 1 contains approximately ~1.3 mg of actinides and is prepared to measure the cross section of  $^{244}\text{Cm}$  whereas sample 2 is prepared to measure the cross section of  $^{246,248}\text{Cm}$  containing approximately ~1.8 mg of actinides. The total masses of the samples are not known precisely, whereas the relative abundances are known with small uncertainties, as presented in Table 1. For this reason, the normalization has been performed to the first resonance of  $^{240}\text{Pu}$ .

**Table 1.** Isotopic abundances (per cent) during the Cm campaign, in August 2017.

Isotope	$t_{1/2}$ (years)	Sample 1	Sample 2
$^{240}\text{Pu}$	6561	$30.8 \pm 0.6$	$9.2 \pm 0.2$
$^{243}\text{Am}$	7364	$0.6 \pm 0.1$	$1.2 \pm 0.2$
$^{244}\text{Cm}$	18.11	$59.9 \pm 1.1$	$20.1 \pm 0.4$
$^{245}\text{Cm}$	8423	$2.4 \pm 0.3$	$1.0 \pm 0.3$
$^{246}\text{Cm}$	4706	$6.3 \pm 0.3$	$57.0 \pm 1.2$
$^{247}\text{Cm}$	$1.56 \cdot 10^7$	-	$2.8 \pm 0.4$
$^{248}\text{Cm}$	$3.48 \cdot 10^5$	-	$8.7 \pm 0.2$

## 2.1 The measurement at EAR1

At EAR1 sample 1 was measured to obtain the resonance parameters of  $^{244}\text{Cm}$  up to 100 eV [8]. The TAC detector used in the experiment consists of 40 BaF<sub>2</sub> crystals covering ~95% of the solid angle [9]. In order to extract the

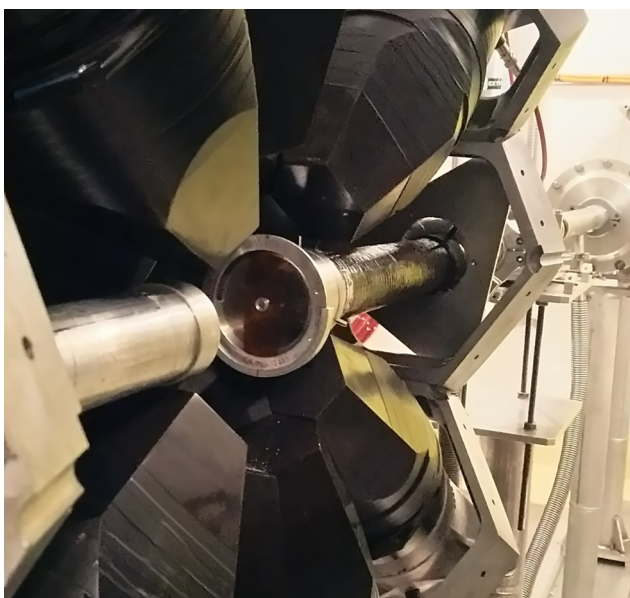


**Figure 2.** Picture of the TAC detector and the sample 1. In the image only one of the semispheres is visible.

neutron yield the following equation is used:

$$Y_{\gamma,exp} = \frac{C - B}{\varepsilon \cdot \phi_n} \quad (1)$$

where  $C$  is the total counting rate,  $B$  is the background counting rate,  $\varepsilon$  is the capture detection efficiency and  $\phi_n$  is the number of neutrons impinging in the sample per unit of time.

In order to reduce the background, the analyses were performed using coincidences between the crystals defining events. The cuts applied in the events are deposited energy sum  $2.5 < E_{sum}(\text{MeV}) < 6$  and the number of crystals recording signals in the event higher than 2. The efficiency to detect the cascades with these analyses cuts are  $0.589 \pm 0.07$  for  $^{240}\text{Pu}$  and  $0.588 \pm 0.07$  for  $^{244}\text{Cm}$ , these values were determined with the cascades obtained with NuDEX and Geant4 simulations [10–12]. The uncertainty obtained in the normalization to the first resonance of  $^{240}\text{Pu}$  considering also the uncertainties in the abundances is 3.3%. Also, the uncertainties in the neutron fluence and the background subtraction were considered in the yield determination.

## 2.2 The measurements at EAR2

At EAR2 samples 1 and 2 were measured to obtain the resonance parameters from  $^{244,246,248}\text{Cm}$ . Three BICRON C<sub>6</sub>D<sub>6</sub> detectors [13] were placed at 5 cm from the sample, see Figure 3. The yields were obtained with the To-

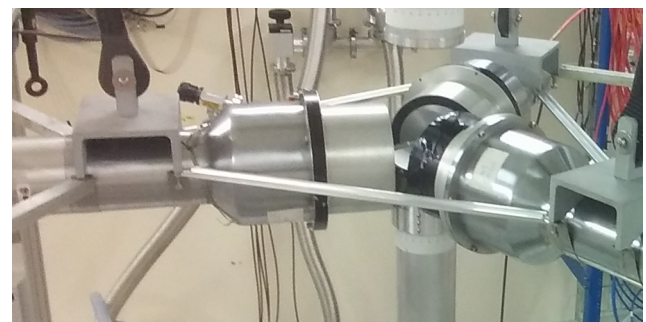


**Figure 3.** Picture of the three BICRON C<sub>6</sub>D<sub>6</sub> used in the experiment. The sample is in the middle of the three detectors at 5 cm from them

tal Energy Detection (TED) and Pulse Height Weighting technique (PHWT) [14]. A weighting function is used to weight each detected count with an energy (pulse height) factor to fulfil the necessary conditions of the TED technique. The equation to obtain the yields with these techniques is:

$$Y_{\gamma,exp,i} = F_{PHWT,i} \frac{C_w - B_w}{S_{n,i} \cdot \phi_n} \quad (2)$$

where  $C_w$  is the total weighted counting rate,  $B_w$  is the background weighted counting rate,  $S_{n,i}$  is the neutron separation energy of the isotope  $i$ ,  $F_{PHWT,i}$  is the factor for correcting the deviations from the ideal situation with the PHWT, and  $\phi_n$  is the number of neutrons impinging

in the sample per unit time. In order to reduce the uncertainties, the unweighted yield would be used normalized to the weighted one using the technique described in reference [15].

The  $F_{PHWT,i}$  factors are determined with Monte Carlo simulations using the  $\gamma$ -ray cascades fitted with NuDEX. The factors consider the counts lost below the detection threshold of 0.12 MeV, the effect of detecting various  $\gamma$ -rays of the cascade or the same  $\gamma$ -ray in various detectors and the  $\gamma$ -ray summing effect. In Table 2 the correction factors for each isotope are presented. The uncertainties in these factors, the normalization, the neutron fluence and the background subtraction were considered in the determination of the yields.

**Table 2.** The  $F_{PHWT}$  to correct the deviations from the PHWT theory for different isotopes and a 0.12 MeV threshold. The uncertainties in the table are derived from the statistics in the Monte Carlo simulations.

Isotope	$^{240}\text{Pu}$	$^{244}\text{Cm}$	$^{246}\text{Cm}$	$^{248}\text{Cm}$
$F_{PHWT}$	1.098(1)	1.134(1)	1.170(1)	1.089(1)

### 3 Resonance analysis of the capture yields

The three capture yields obtained in EAR1 and EAR2 with the two samples have been analysed to obtain the Resonance Parameters (RP) of the  $^{244,246,248}\text{Cm}$  and  $^{240}\text{Pu}$  isotopes in the Resolved Resonance Region (RRR). The resonances have been fitted with SAMMY [16], a code widely used in the nuclear data community, applying the R-matrix formalism and the Reich-Moore approximation [17]. The different experimental effects consider in the SAMMY analysis are:

- The Doppler broadening is caused by the thermal motion of the target nuclei. In this experiment, the free gas model has been used.
- The multiple scattering effects, which take into account that the neutrons can be captured after one or more elastic scatterings. SAMMY calculates this effect by performing dedicated Monte Carlo simulations.
- The resolution broadening is caused by the different TOF of the neutrons of the same energy arriving at the sample. The time-energy distribution of the neutrons is given by the resolution function (RF). In EAR1 the standard RF was taken [6], whereas for EAR2 it was necessary to calculate a particular RF for the experiment fitting the resonances of  $^{197}\text{Au}$  [18].

The  $E_n$  and  $\Gamma_n$  parameters of  $^{244,246,248}\text{Cm}$  and  $^{240}\text{Pu}$  has been obtained for different energy regions. The rest of the RP ( $\Gamma_f$ ,  $\Gamma_\gamma$  and spin) are taken from the JENDL-4 library [19]. As an example in Figures 4 and 5 the fits performed for the first resonances of each isotope are presented. The energy ranges analysed for each isotope are presented in Table 3. For the first time at n\_TOF a capture measurement has been performed at EAR1 and EAR2 with different detection setups, as presented in Figure 6. The results

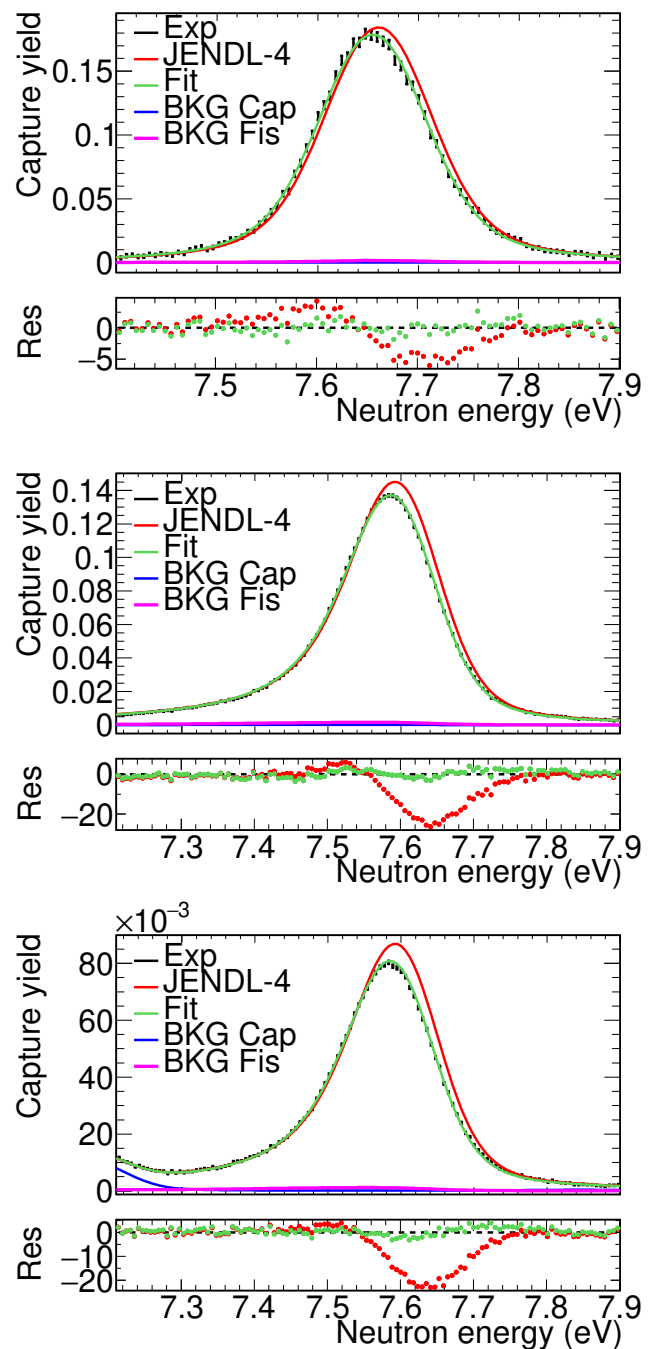


**Figure 4.** Experimental  $^{244}\text{Cm}$  capture yields close to the resonances at 7.67 eV (black) compared with the yield obtained with the JENDL-4.0 data (red) and with the yield obtained with the fit (green). In blue, the calculation of the background due to the other actinides and in pink the fission background. The top figure is the yield obtained in EAR1 with sample 1. The middle and bottom figures are measurements in EAR2 the first one with sample 1 and the second one with sample 2. The bottom panel of each Figure are the residuals.

obtained in both areas and with two different samples are compatible validating the analysis performed in EAR2.

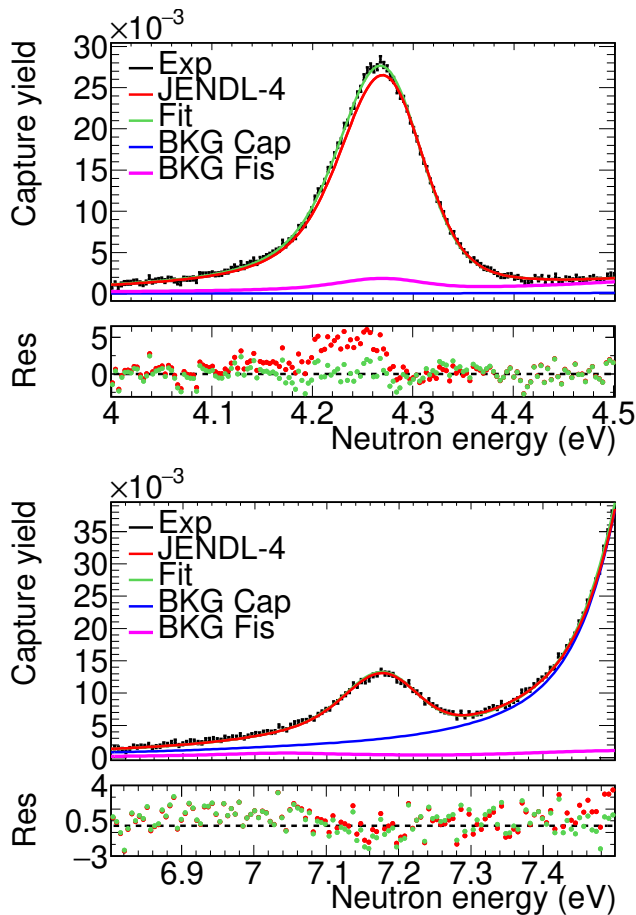


**Figure 5.** Experimental  $^{246}\text{Cm}$  (top) and  $^{248}\text{Cm}$  (bottom) capture yields close to the first resonances (black) at 4.3 and 7.2 eV respectively compared with the yield obtained with the JENDL-4.0 data (red) and with the yield obtained with the fit (green). In blue, the calculation of the background due to the other actinides and in pink the fission background. The bottom panel of each Figure are the residuals.

**Table 3.** The energy regions fitted to obtain RP for the different isotopes in the experiments performed in the different areas with various samples.

Area	EAR1	EAR2	EAR2
Sample	1	1	2
$^{240}\text{Pu}$	20-100 eV	20-200 eV	20-150 eV
$^{244}\text{Cm}$	7-100 eV	7-300 eV	7-250 eV
$^{246}\text{Cm}$	-	-	4-400 eV
$^{248}\text{Cm}$	-	-	7-100 eV

## 4 Summary and conclusions

This work presents a series of measurements of the capture cross section of  $^{244,246,248}\text{Cm}$  from 1 to 400 eV using two complementary experimental areas of the n\_TOF facility and different samples to improve the present evaluations. The experiment was the first capture measurement at n\_TOF performed in the two experimental areas, also for the experiments, two different setups were used (TAC and  $\text{C}_6\text{D}_6$  detectors). The efficiencies and the different corrections needed were obtained considering the cascades ob-

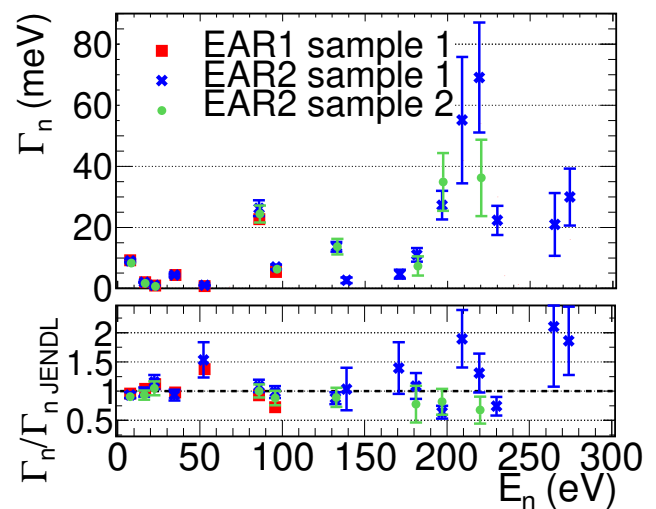


**Figure 6.**  $\Gamma_n$  values obtained in the three measurements of the  $^{244}\text{Cm}$  RP compare with the JENDL-4 evaluation. For energies below 50 eV the three measurements are compatible with JENDL-4 and the discrepancies with this evaluation are less than 15%.

tained with NuDEX, these accurate work leads to small uncertainties in the absolute yields. The results obtained in the two areas with different detectors are compatible. The work that is already ongoing is to combine the information of the various measurements to obtain the final RP with their corresponding uncertainties, these results will be published in dedicated papers and sent to the EXFOR database.

## 5 Acknowledgments

This work was supported in part by the I+D+i grant PGC2018-096717-B-C21 funded by MCIN/AEI/10.13039/501100011033 and by the European Commission H2020 Framework Programme project SANDA (Grant agreement ID: 847552).

## References

- [1] G. Aliberti et. al., , Ann. Nucl. Ener. 33, 700 (2006)
- [2] Croff, A.G. Nucl. Technol., 62(3), 335-352 (1983)
- [3] M. S. Moore et. al., Phys. Rev. C, 3, 1656 (1971)
- [4] A. Kimura et. al., Jour. Nucl. Sc. Tech. 49, 708 (2012)
- [5] S. Kawase et. al., Jour. Nucl. Sc. Tech. 58:7, 764-786 (2021)
- [6] Guerrero, C. et al. Eur. Phys. J. A 49, 27 (2013)
- [7] C. Weiss et al., Nucl. Instrum. Meth. A 799, 90 (2015)
- [8] V. Alcayne et al., EPJ Web Conf., 239 01034 (2020)
- [9] C. Guerrero et al., Nucl. Instrum. Meth. A 608, 424 (2009)
- [10] S. Agostinelli et al., Nucl. Instrum. Meth. A 506, 250 (2003)
- [11] E. Mendoza et al., EPJ Web Conf., 239 01015 (2020)
- [12] E. Mendoza et al., EPJ Web Conf., 239 17006 (2020)

- [13] R. Plag *et al.*, Nuc. Inst. Meth. A. 496 2, 425-436, (2003)
- [14] U. Abbondanno *et al.*, Nuc. Inst. Meth. A. 521, 454-467, (2004)
- [15] J. Leredegui-Marco *et. al.*, Phys. Rev.C 97, 024605 (2018)
- [16] N.M. Larsson. Updated User's Guide for SAMMY. Technical report, ORNL, (2006)
- [17] C. W. Reich and M. S. Moore. Phys. Rev., 111:929–933, (1958)
- [18] V. Vasilis. On the resolution function of the n\_TOF facility. Technical CERN report: 2764434 (2021)
- [19] K. Shibata *et. al.*, Jour. Nucl. Sc. Tech. 48 (1):1–30, (2011)